CanmetMATERIALS

Characterization of Microstructure, Tensile (23°C to 850°C) and Charpy Transition Curves of a Current Tank Car Steel (TC128B) Circumferential Weld

S. Xu, J. McKinley, J. Chen, J. Liang and A. Laver

Report No. CMAT-2018-WF 34540443
TP 15515E
Catalogue No. T86-74/2022E-PDF
ISBN: 978-0-660-42411-8

January 2019

CMAT

DISCLAIMER

Natural Resources Canada makes no representations or warranties respecting the contents of this report, either expressed or implied, arising by law or otherwise, including but not limited to implied warranties or conditions of merchantability or fitness for a particular purpose.

CanmetMATERIALS

REPORT CMAT-2018-WF 34540443

CHARACTERIZATION OF MICROSTRUCTURE, TENSILE (23°C TO 850°C) AND CHARPY TRANSITION CURVES OF A CURRENT TANK CAR TC128B STEEL CIRCUMFERENTIAL WELD

by

S. Xu, J. McKinley, J. Chen, J. Liang and A. Laver

EXECUTIVE SUMMARY

This report details experimental procedures and results of microstructure, tensile and Charpy properties of a current TC128B circumferential weld. The sample coupon was received from at DOT-117 tank car. The work included the determination of (i) chemical composition, microstructure and micro-hardness (ii) tensile strength and failure locations in the temperature range of 23°C to 850°C, and (iii) Charpy transition curves.

The weld was made using a double pass procedure. The combined weld and heat affected zone (HAZ) widths were approximately 14.8 mm close to the mid-thickness (the smallest), 22 mm at the inside surface and 24 mm at the outside surface (the largest), respectively. The HAZ width ranged approximately 2.3-4.2 mm. Weld metal (WM) and HAZ showed typical microstructures. The hardness values in the weld and HAZ were considerably higher than those of base metal (BM), i.e., demonstrating desired weld strength over-matching. The average and standard deviation of micro-hardness of BM, HAZ and WM were 164±8 (from 152 to 182), 191±17 (from 151 to 217) and 194±9 (from 163 to 217), respectively. Ultimate tensile strength (UTS) of cross-weld tensile specimens dropped sharply beyond 600°C as it did in all BM tests performed previously. All cross-weld specimens tested at 700°C and below failed at the BM. Two of the spciemens tested at 700°C and one specimen tested at 800°C broke close to the weld region (probably in HAZ). Two cross-weld tensile specimens at 800°C failed in the WM. At 850°C, three cross-weld tensile specimens failed in BM. These indicated that the WM may become a weak link at high-temperatures approximately above 700°C to 800°C. However, in all cases, the UTS of the specimens were similar no matter where the specimen failure occurred. CVN (Charpy V-notch) values of WM were significantly lower than those of BM. CVN values of HAZ specimens were between those of BM and WM, and displayed larger scatter. CVN values for WM specimens at -46°C (average: 18 J, individual: 16 J, 24 J, 13 J) indicated that the weld toughness values were slightly lower than the specified values (i.e., 20.3 J minimum average for three specimens and 13.6 J minimum for one specimen at -46°C). The cross-weld tensile and Charpy test results indicated a need to optimize the current welding procedure.

The low toughness of the weld metal (CVN values) should be investigated further. CanmetMATERIALS's recommended course of action is to begin by verifying these results by testing another weld from the same tank car (e.g., a longitudinal weld). Additional welds from tank cars manufactured with TC 128B steels should be tested. This should be followed by reviewing the standard practice for TC128B welding and then development of an improved weld process. It may be possible to improve the weld toughness using minor changes to the welding parameters, heat treatment, or filler metal composition without making significant changes to existing procedures and equipment.

CONTENTS

1. INTRODUCTION

A rail tank car is an important method of transporting bulk liquid chemicals, including dangerous goods such as propane, ammonia, vinyl chloride, ethylene oxide, alcohol and petroleum oil/gases [1]. TC128B is currently the most common steel used in the manufacturing of tank cars. In the event of a rail tank car accident whilst transporting flammable liquids, there is a potential for a pool fire. The fire may subject a portion of the steel tank car to localized heating; in the event of an engulfing fire, the entire car is involved. Tank car may also experience low temperatures in service. , Material properties at temperatures up to 816°C for the fire pool analysis or for the torch fire analysis at 1205°C are of interest [2,3] while the lowest design temperature in Association of American Railroads (AAR) specification is -46°C (or 50°F) [3]. In addition to materials properties of tank car steel, the properties of steel welds are critical to the integrity of the tank car because tank cars are fabricated using welding techniques.

In this work, a current tank car TC128B circumferential weld was characterized to examine the microstructure, hardness, tensile and Charpy impact ductile-to-brittle transition properties. Cross-weld (or also referred to as transverse tensile) and all-weld-metal tensile tests were performed to evaluate the weld joint performance, i.e., whether the weld is a weak location for failure and its strength is lower than the base shell steel [2,4] or not. Charpy toughness tests of the weld metal (WM) and heat-affected zone (HAZ) were performed to establish Charpy transition curves. Weld metal consists of solidified dendritic microstructures and usually contains hard phases and the weld strength is usually higher than that of base metal. The transition temperature of the welds may be higher than the base metal (BM) which would lead to an increased risk of failure in the weld area in cold environments. This report summarizes material test results, experimental procedures and results of characterizations.

2. MATERIAL AND EXPERIMENTAL PROCEDURES

The tank car TC128B weld samples were taken from a tank car conforming to DOT 117 specifications, fabricated in 2015 and subjected to a side-impact test in September 2016. The tank car was purchased and the impact test was sponsored by the United States Department of Transportation (DOT). The shell has a nominal thickness between 12.7 mm (9/18″) to 15.9 mm (10/16″). The tank car was fabricated using a submerged arc welding process. From locations sufficiently far away from the impact location, plates with and without welds were sectioned and provided to CanmetMATERIALS for testing. Figure 1 shows post-impact-test photograph of the tank with plate sections. The plate rolling direction (RD) is normal to the axis of the tank. A circumferential weld used in this work is shown in Figure 2. Cross-weld tensile specimens were taken transverse to the weld length and at transverse direction (TD) of the steel plate. The steel thickness was approximately 14.8 mm close to the weld.

Figure 1. US Federal Railroad Administration impact-tested tank car, showing location of TC128B panel used in this work. Photo provided by Nolan Hanson of the Transportation Technology Center, Inc.

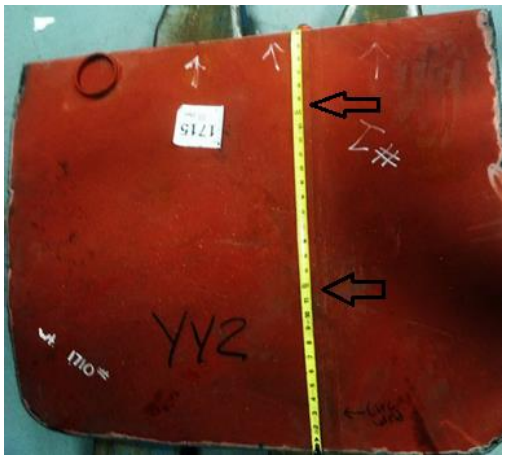

Figure 2. Tank car TC128B circumferential weld.

The compositions of the tank car steel (from [4]) and WM were analyzed using optical emission spectroscopy and are given in Table 1. The chemical composition specifications for the TC128B [3] are listed in Table 1 for reference. The composition meets the ARR 2014 specification for TC128B [3]. The low Sulfur (S) and Phosphorus (P) contents of the BM are consistent with the current clean steel making technology. The weld was considered to have higher carbon content (typical less than 0.08%) and oxygen (0.0826%) than typical submerged arc welding (SAW) (~up to 0.05%) [6] and lower ratio of Ti/N (1.6) than that of the BM (2.3).

Table 1. Chemical composition of the steel [4], limits for TC128B (wt%) [3] and weld

Element	Spectroscopy analysis of BM sample	TC128B, maximum permitted in product analysis [3]	Spectroscopy analysis of WM sample
C	0.19	0.26	0.18
Mn	1.34	1.00-1.70	1.54
P	0.0059	0.25	0.0182
S	0.0014	0.009	0.0117
Si	0.16	0.13-0.45	0.35
V	0.034	0.084	0.016
Cu	0.21	0.35	0.18
Al	0.032	0.015-0.060	0.021
Nb	<0.001	0.03 (per ASTM A20 [5])	0.002
Ti	0.0016	0.020	0.0129
B	0.0002	0.0005	0.0004
O		(Not determined)	0.0826
N	0.0069	0.012	0.00831
Sn	0.0112	0.020	0.006
CE*	0.46	0.55	0.53
Nb+V+Ti	<0.0366	0.11	0.031
Cu+Ni+Cr +Mo	0.43	0.65	0.32
Ti/N	0.23	4.0	1.6

* CE=C+(Mn+Si)/6+(Ni+Cu)/15+(Ni+Mo+V)/5

Transverse weld metallographic specimens with the weld reinforcement were cut using a water-jet machine for microstructural and micro-hardness characterization. Metallography was performed using standard polishing procedure and etched using 2% Nital. Secondary electron microscopy (SEM) was used to help in resolving fine structures. Vickers micro-hardness tests were performed using a diamond pyramid indenter with a load of 300 gram-force and a dwell time of 10 seconds. The hardness values (H_v) were measured across the weld at three through-thickness positions: (i) ~2 mm from the tank outside surface; (ii) at the mid-wall thickness; and (iii) ~2 mm from the tank inside surface.

Transverse tensile tests were carried out to evaluate weld performance of TC128B tank car at different temperatures. According to AAR specification [3], two full-thickness rectangular cross-weld tensile specimens with a gauge length of 50.8 mm (Figure 3) were tested. The weld reinforcement on both sides of the rectangular cross weld tensile specimen were removed by milling. Figure 4 shows the cylindrical tensile specimen geometry used with a gauge length of 50.8 mm and diameter of 6.25 mm. According to AAR specification [3], the reduced section of cross-weld tension specimens should be longer than the width of weld plus two specimen diameters. The use of this sub-size cylindrical tensile specimen was to facilitate testing at high temperatures and to also allow more specimens for a given length of the weld. Cylindrical tensile specimens were machined from the middle-thickness of the weld. All tests were performed at a quasi-static rate and at temperatures between 23°C and 850°C. For high-temperature tensile tests, the specimens were heated to the test temperatures and were held at the required temperature for 30 min before testing. At 800°C, the time required to heat the specimen was

about 2 hours. Two cylindrical all-weld-metal (AWM) specimens with a gauge length of 25.4 mm and diameter of 6.35 mm were taken along the weld close to the middle-thickness to measure WM properties to compare to the specification requirements.

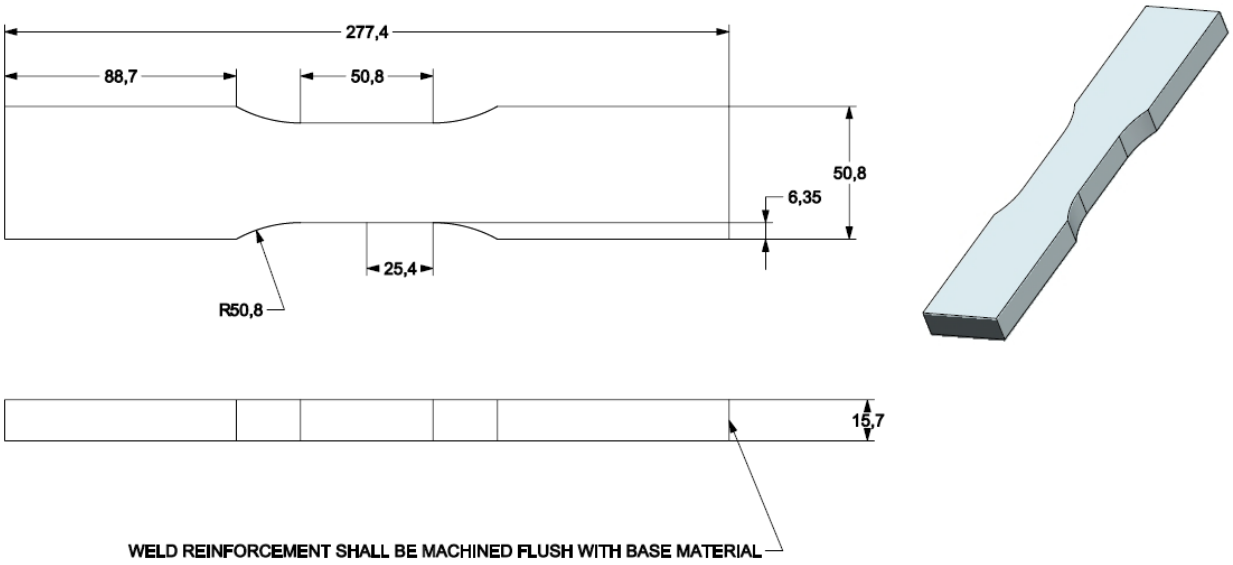

Figure 3. Transverse rectangular cross weld tensile specimen according to AAR specification [3]. Dimensions in mm.

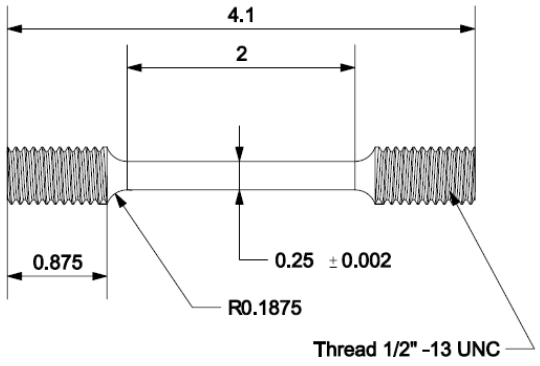

Figure 4. Cylindrical tensile specimen. Dimensions in inch.

Charpy V-notched specimens were prepared according to AAR specification [3]. Charpy specimen location and orientation for tank car WM and HAZ are shown in Figure 5 [3]. Charpy specimen notch was placed through thickness. Charpy specimens were taken close to the outside surface as possible.

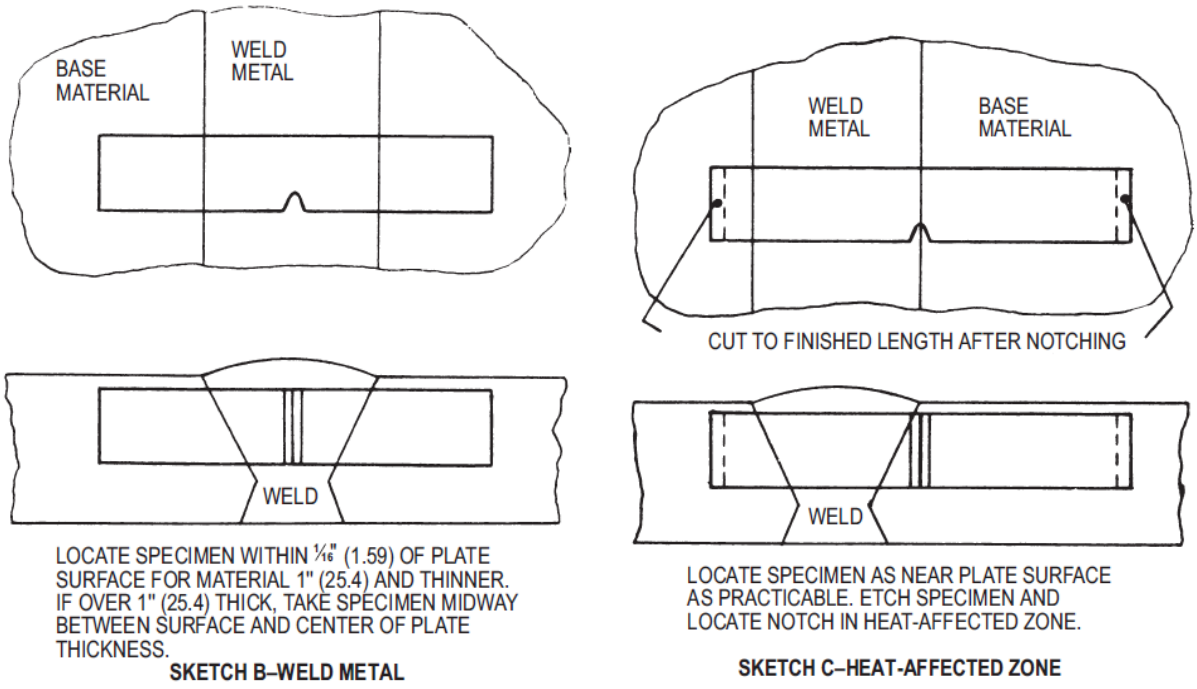

(a) WM (b) HAZ

Figure 5. Charpy specimen location and orientation for tank car WM and HAZ according to AAR specification [3].

3. RESULTS AND DISCUSSION

In order to examine general characteristics of the TC128B circumferential weld, and assist mechanical specimen preparation, metallography, micro-hardness and micrography were performed and are described. Mechanical properties of the tank car steel weld were evaluated and are compared to those of BM.

3.1 Macrography of Weld

A macrography of current TC128B circumferential weld is shown in Figure 6. The macrography shows that the weld was made using a double pass SAW procedure[1], which is a normal mechanized welding procedure for TC128B tank cars [7]. The first-pass (or root pass) weld was made from the inside surface and the WM height was about 1/3 of the weld thickness while the second-pass (or cap pass) weld completed the joining. The first-pass and second-pass welds were aligned well. The combined weld and HAZ widths were approximately 14.8 mm close to the mid-thickness (the smallest), 22 mm at the inside surface and 24 mm at the outside surface (the largest), respectively. The HAZ width ranged approximately 2.3-4.2 mm. There was a doubly tempered HAZ between the first-pass and second-pass WMs in the weld overlap region which is the lightly gray region in Figure 6; this reheated (RH) WM

[1] A submerged arc weld procedure was used to fabricate the tank car.

region was, as expected, significantly influenced by the re-heating of the second-pass weld as will be shown in micrographs in Subsection 3.3. The height of RH WM zone is approximately 1.2 mm at the centerline and the height of the weld was approximately 17.2 mm. The RH WM is approximately 7% of WM. The bay region indicated in Figure 6 will be discussed in the next two subsections.

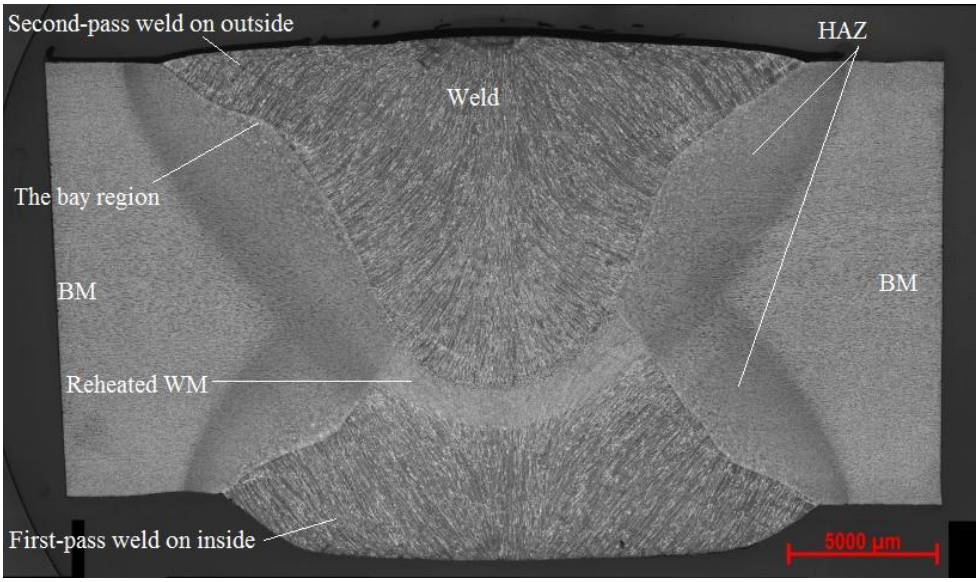

Figure 6. Macrography of TC128B circumferential weld.

3.2 Micro-hardness Across Weld

Micro-hardness measurements were made across the weld specimen and the hardness indentations (black dots) are shown in Figure 7. Twenty through-thickness micro-hardness tests were also performed on a section of tank car base metal (BM) and showed good consistent results 164±8 (from 152 to 182; the ratio of standard deviation to average was 4.6%). Cross-weld micro-hardness measurements are shown in Figure 8 and the average BM hardness (164) is shown as a horizontal dash-line for comparison. The regions of BM, HAZ and WM were illustrated in Figure 8a-c based on the indentation locations in Figure 7. The origin of X-axis in Figure 8 corresponded to the first hardness measurement on the right side in Figure 7. Since fusion line and HAZ boundaries at the three through-thickness positions are different these boundaries in Figure 8d are not illustrated. The average and standard deviation of micro-hardness of HAZ as measured in three through-thickness positions were 191±17 (from 151 to 217) and these of WM were 194±9 (from 163 to 217). The highest hardness values in the weld and HAZ were 217. The six hardness measurements in the RH-WM close to WM centerline yielded values of 185±3 (from 181 to 191), which are higher than the BM (avg. 185 vs. 163) but slightly lower than WM (avg. 185 vs. 194) and HAZ (avg. 185 vs. 191) hardness values. The main observation from the measurements was that the hardness values in the weld and HAZ were considerably higher than those of BM, i.e., demonstrating desired weld strength over-matching. The hardness values in the HAZ at 2 mm below the outside surface close to the second-pass weld fusion line (so-called the bay region in Figure 6) were slightly higher than those in the other two thickness positions (Figure 8d). The bay region close to the fusion line in the final weld pass usually displays coarse grained microstructure due to fast cooling rate after welding (e.g., [8]).

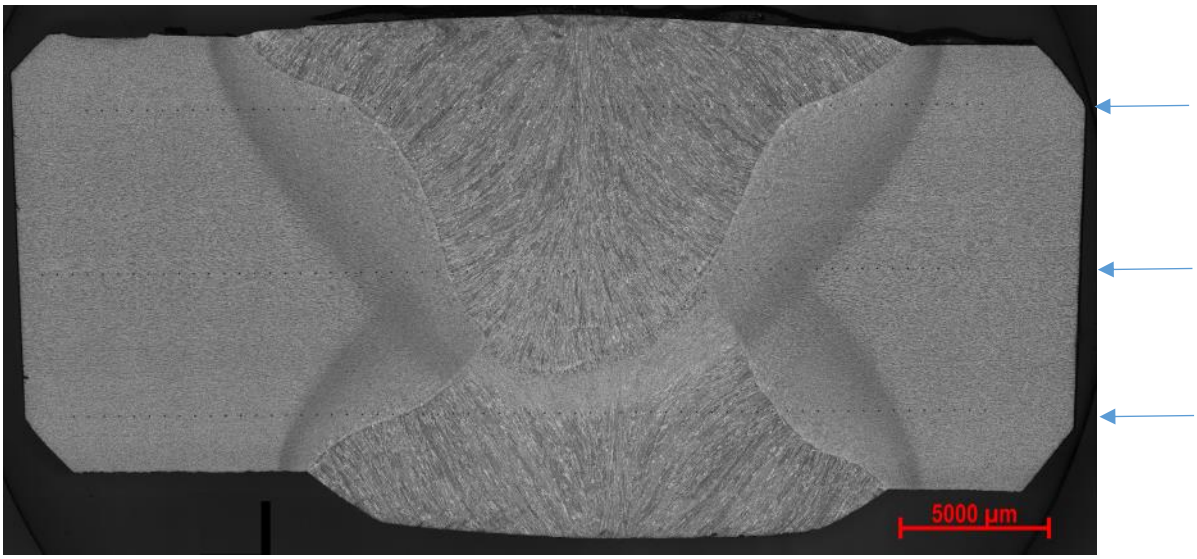

Figure 7. Macrography of cross-weld micro-hardness measurement positions.

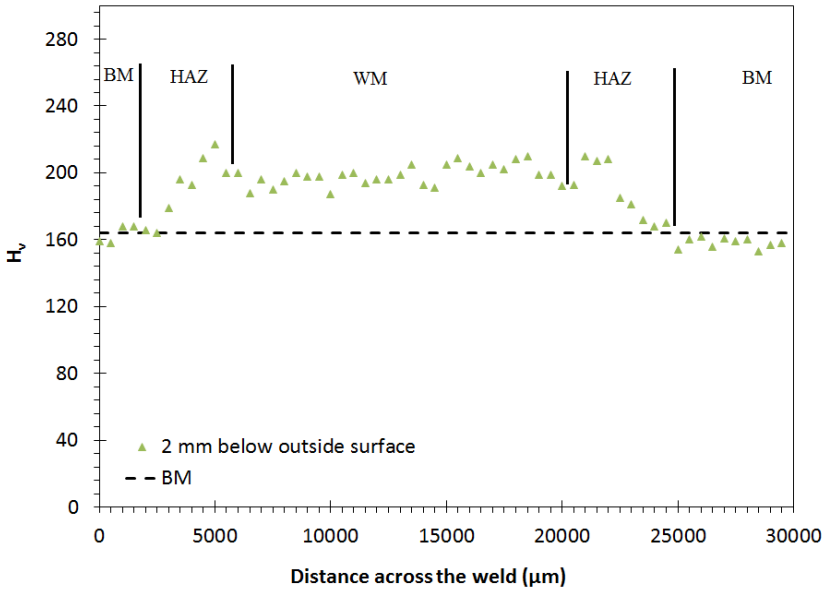

(a) Micro-hardness measured at 2 mm below outside surface

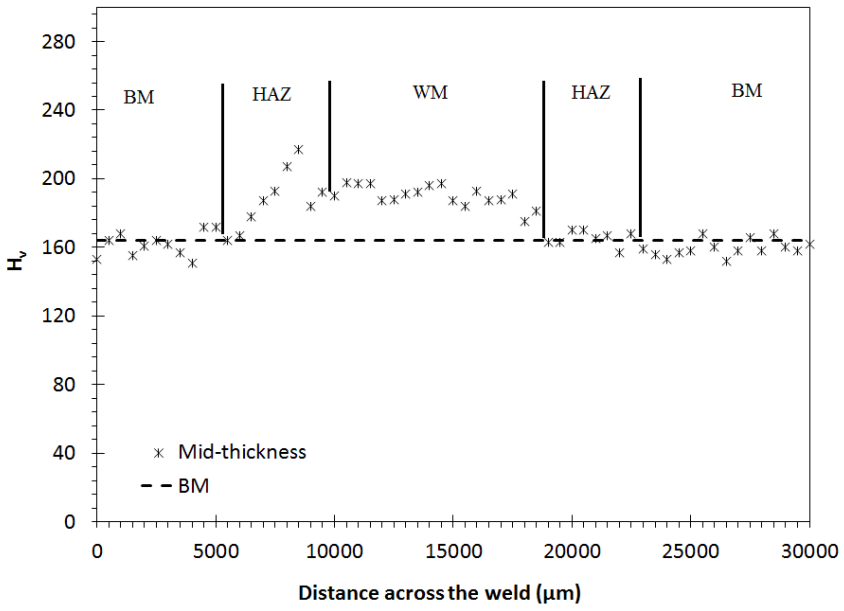

(b) Micro-hardness measured at mid-thickness

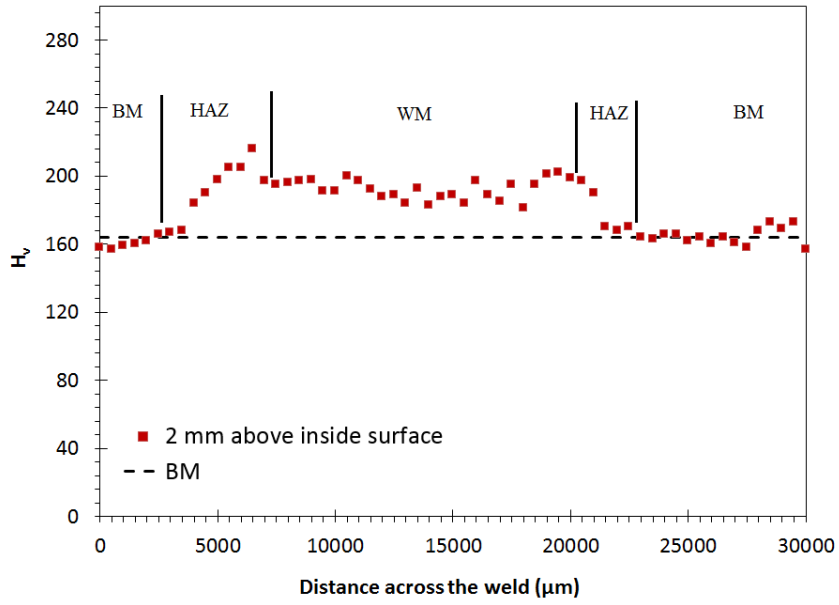

(c) Micro-hardness measured at 2 mm above inside surface

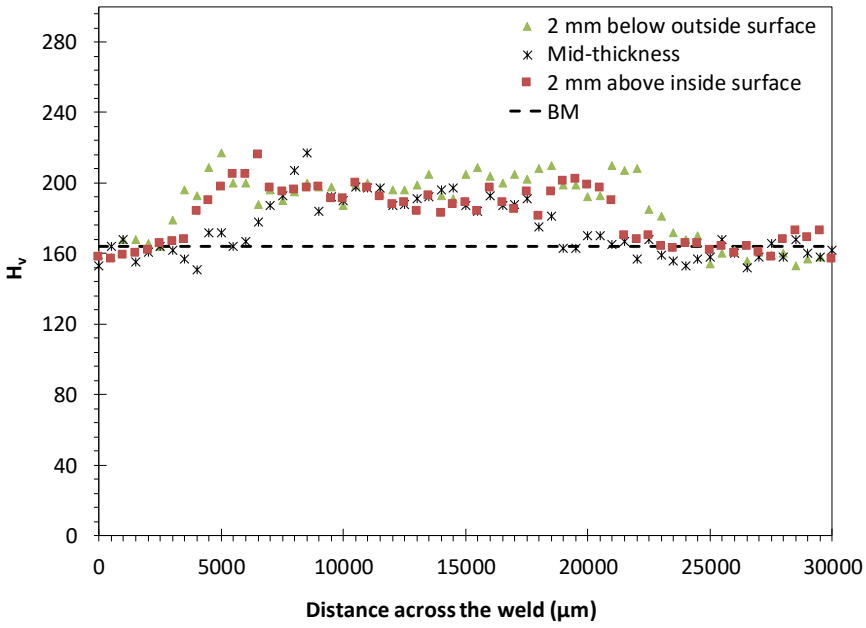

(d) Combined micro-hardness profile

Figure 8. Micro-hardness across the TC128weld.

3.3 Microstructure

Microstructure is one key determinant of the final mechanical properties of HAZ and weldment. A detailed description of the HAZ formation and associated phase transformation and quantitative microstructural characterization are beyond the scope of this work. The following brief description is provided as basis for presentation of results. A schematic representation of microstructure developed in HAZ is shown in Figure 9 [9] (originally from [10]). According to [9,10], the microstructure of HAZ includes (i) coarse grain region (CGHAZ): Material near the fusion boundary that reaches a temperature well above A_{c3} during welding(refer to Figure 9), (ii) fine grain region (FGHAZ): Away from the fusion boundary where the peak temperature is lower, but still above A_{c3}, (iii) intercritical region (ICHAZ): In this regions, peak temperature is between A_{c1} and A_{c3}, resulting in partial reversion to austenite on heating, and (iv) over tempered region. Note that A_{c1} in Figure 9 is the temperature of starting to transfer to austenite and A_{c3} is the temperature of completing to austenite transformation; the temperatures in Figure 9 may be higher than those for TC128B due to different alloy compositions. Also noted that since 1998, AAR specification (M-128) requires new tank cars to be stress relieved at 649°C (1200°F) for one hour after fabrication (as cited in [11]). The stress relieving treatment slightly decreases the strength, increases or maintains the ductility of TC128B and are beneficial to low-temperature fracture properties [1,12]. As such, the observed weld and HAZ microstructures of TC128B were tempered.

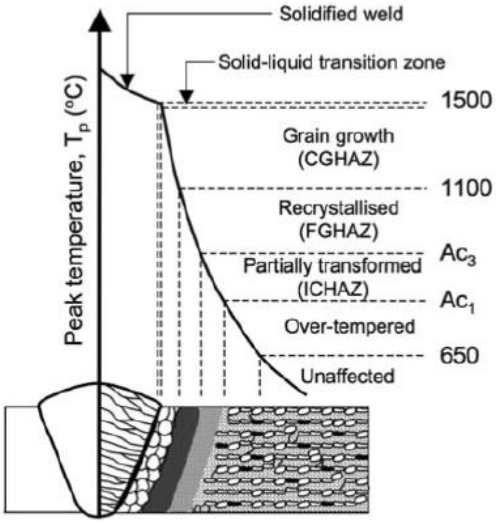

Figure 9. Schematic representation of microstructures developed in HAZ as approximate function of peak temperature during welding [9].

The microstructure of the TC128B circumferential weld region was surveyed. Optical micrographs of typical microstructure of BM and weld region of TC128B were taken. In order to resolve the fine details of the WM and HAZ microstructures, SEM examinations were also carried out. The obtained micrographs are considered typical of TC128B weld region based on the microstructural survey and information in the literature (see e.g., [7,12]). The microstructure of BM has equiaxed grains with grain size approximately 10-20 µm, as shown in Figure 10. The constituent phases are ferrite (white) and pearlite (dark) in a heavily banded structure (Figure 10a). This indicates micro-segregation of Carbon (C) and Manganese (Mn) in the pearlite bands. The BM microstructure is consistent with the results in previous research on the TC128B steel [4]. The pearlite lamellar structure in the BM was revealed using high magnification in a scanning electron microscope (Figure 12b).

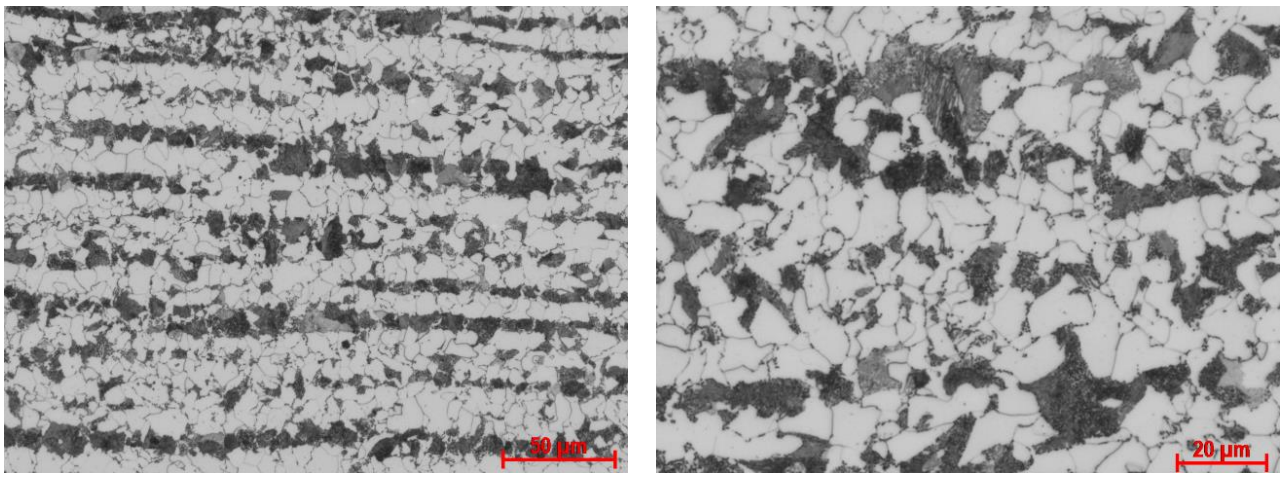

(a) Optical micrographs of BM at ¼ thickness of steel

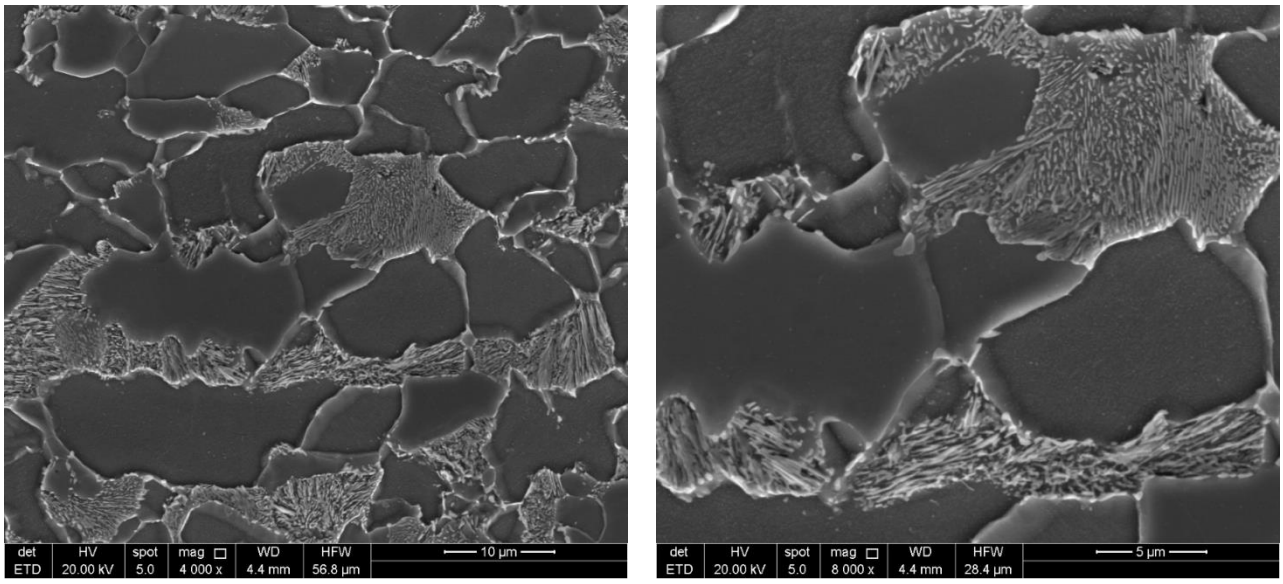

(b) SEM micrograph of BM close to ¼ thickness of steel

Figure 10. Microstructure of TC128B steel (transverse direction).

The microstructure in the weld region including HAZ is more complex than that of the BM. The WM microstructure at the middle of weld centerline in the second-pass is shown in Figure 11. It appeared to consist of coarse proeutectoid ferrite (white) along WM solidification direction, acicular ferrite and/or bainite (grey), and some pearlite (dark). The formation of pearlite in the weld metal indicated that cooling rate after welding was relatively small. As a result, very coarse proeutectoid ferrite was formed with a relative high volume percentage, whereas the volume percentage of acicular ferrite is small. At high magnifications in SEM micrographs, there appeared to be some round inclusions in the WM (white arrows in Figure 11b). However, the composition of microstructural constituents and inclusions (size and distribution) were not analyzed in this work.

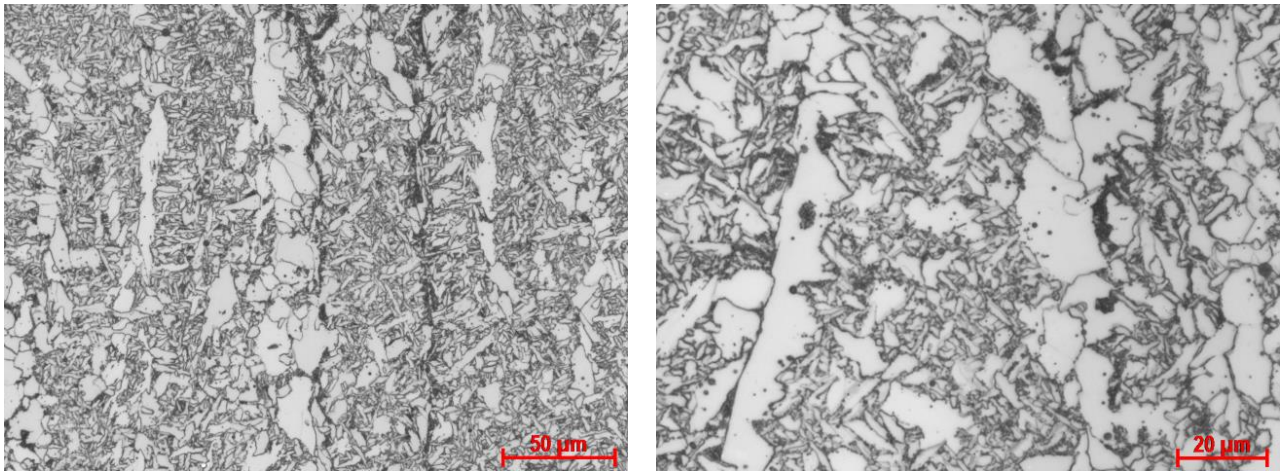

(a) Optical micrograph of WM at the middle of weld centerline in the second-pass

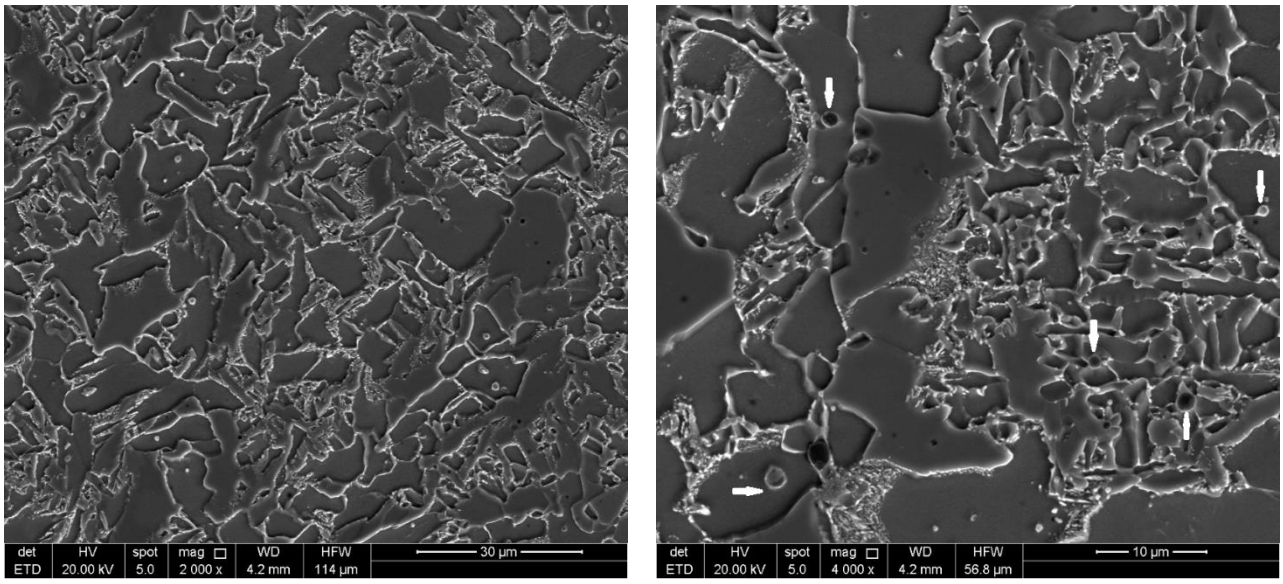

(b) SEM micrograph of WM at the middle of weld centerline in the second-pass

Figure 11. Microstructure of TC128B WM.

In the CGHAZ region close to the bay region as shown in Figure 12a, coarse grain boundary ferrite was present at prior austenite grain boundaries, and within austenitic grains, Widmanstätten ferrite and acicular ferrite and/or tempered bainite and/or tempered martensite were observed (Figure 12b and Figure 12c).

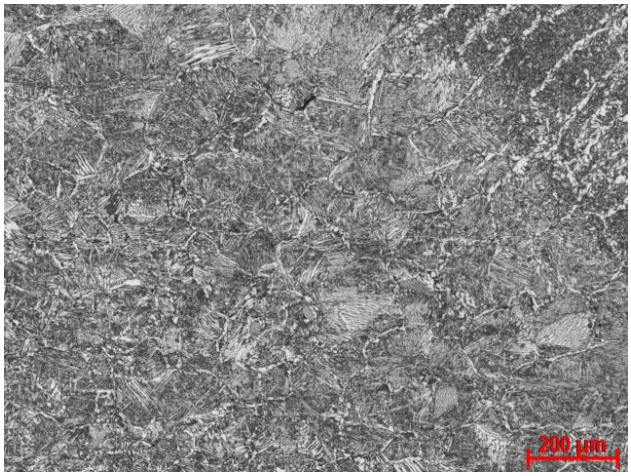

(a) Optical microsgraph of CGHZ and WM in the bay region

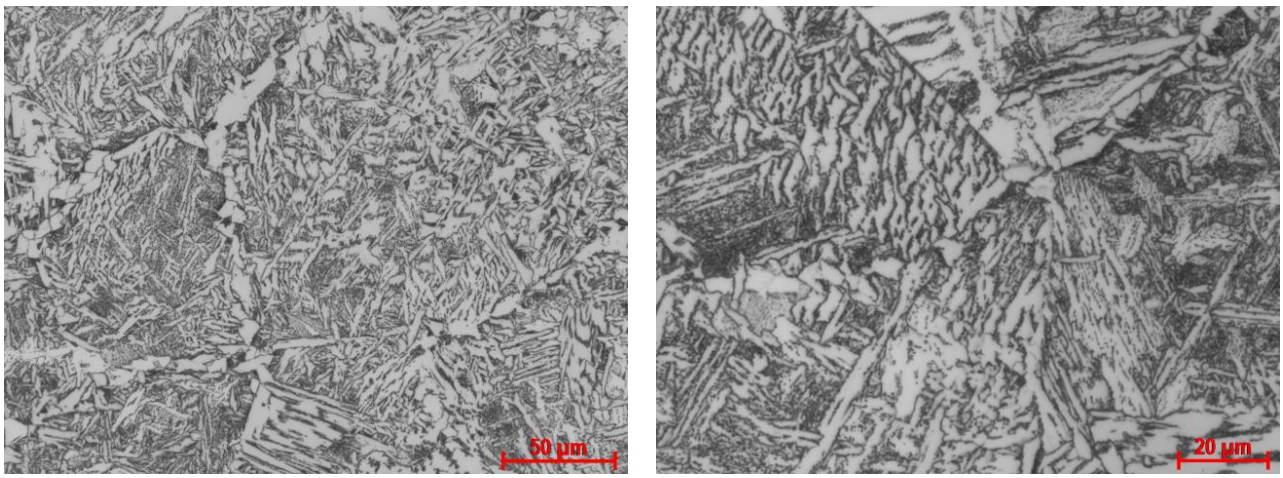

(b) Optical micrograph of CGHAZ in the bay region

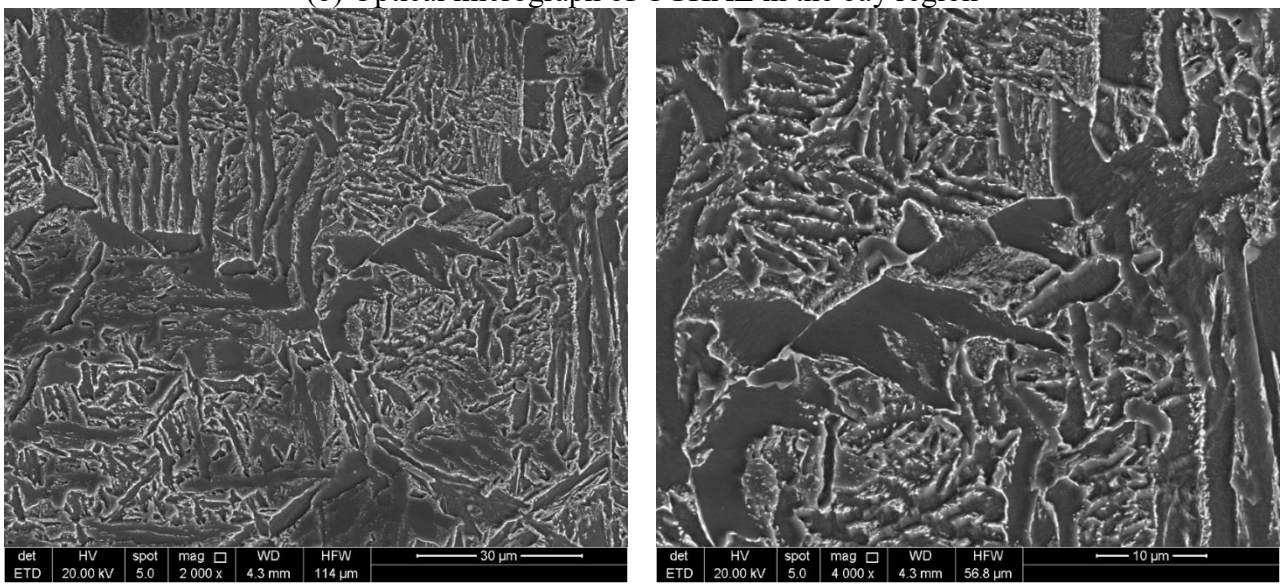

(c) SEM micrograph of CGHAZ

Figure 12. Microstructures of CGHAZ.

The transition region of the FGHAZ and ICHAZ is displayed in Figure 13 and Figure 12a. Microstructures of the FGHAZ (Figure 13b and Figure 13c) and ICHAZ (Figure 13d and Figure 13e) regions close to the mid-thickness of the weld region consisted of fine equiaxed ferrite grains (white), pearlite (dark) and possibly a small amount of tempered bainite/martensite/retained austenite (grey).

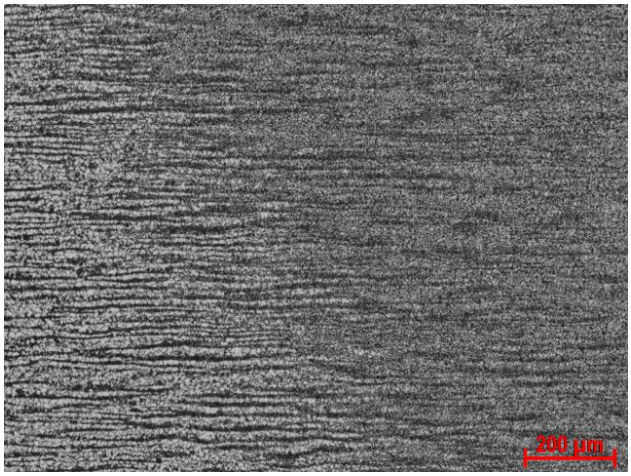

(a) Optical micrograph of FGHAZ and ICHAZ close to mid-thickness of the weld region

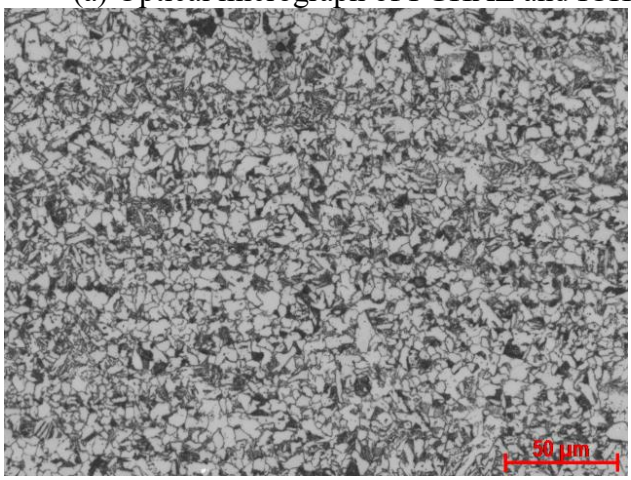

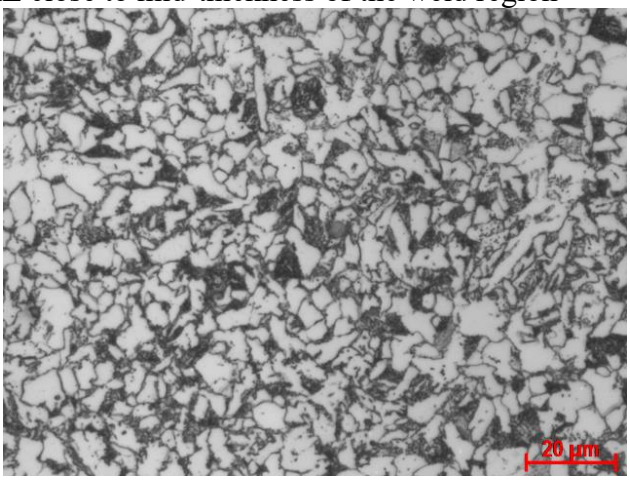

(b) Optical micrograph of FGHAZ close to mid-thickness of the weld region

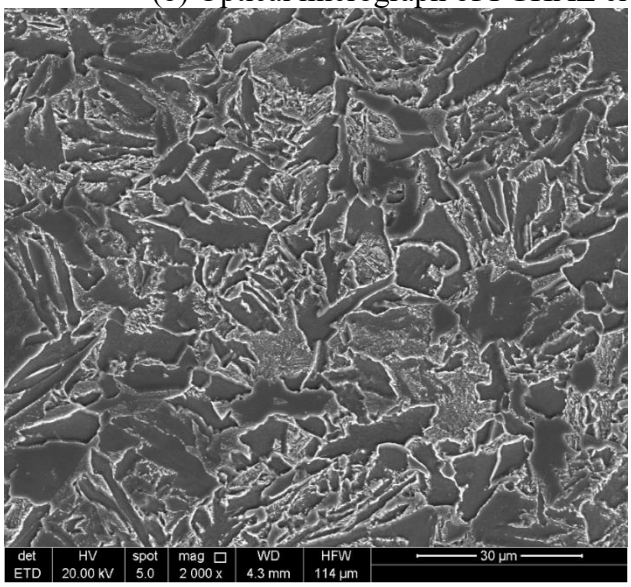

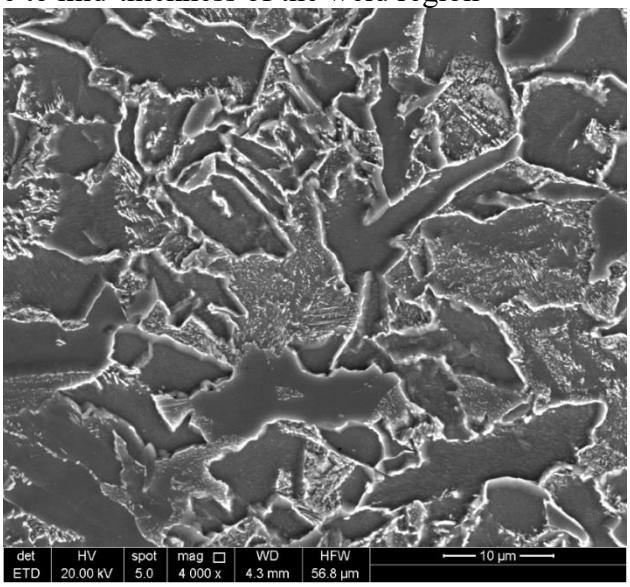

(c) SEM micrograph of FGHAZ close to mid-thickness of the weld region

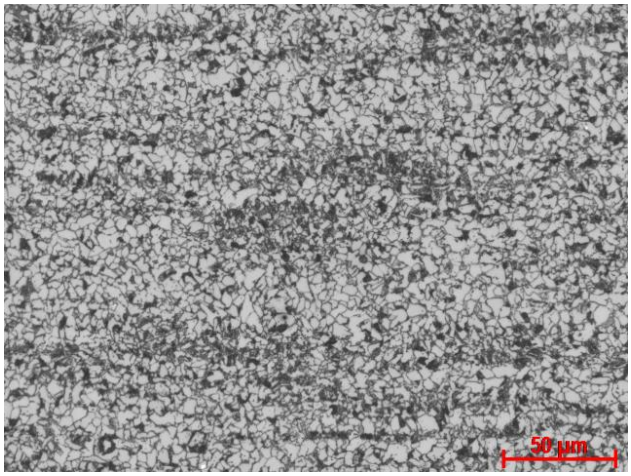

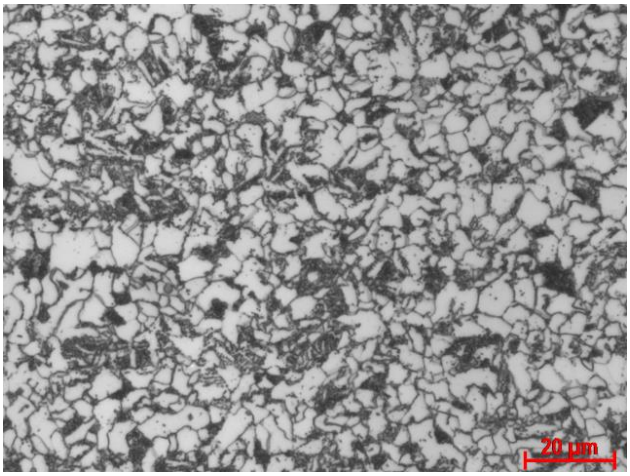

(d) Optical micrograph of ICHAZ close to mid-thickness of the weld region

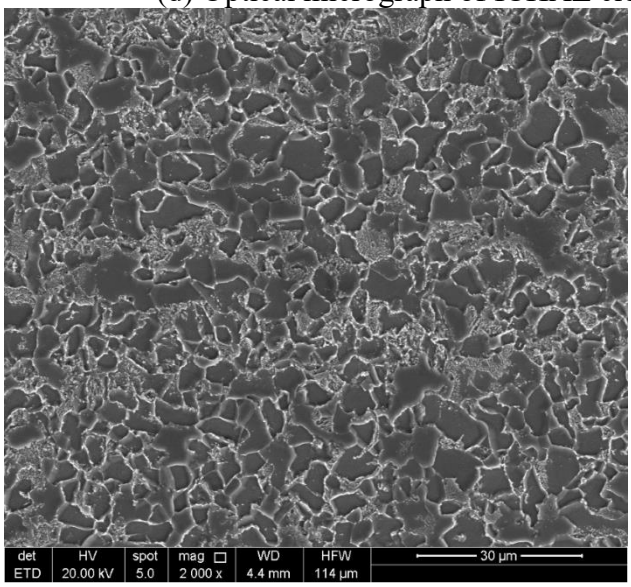

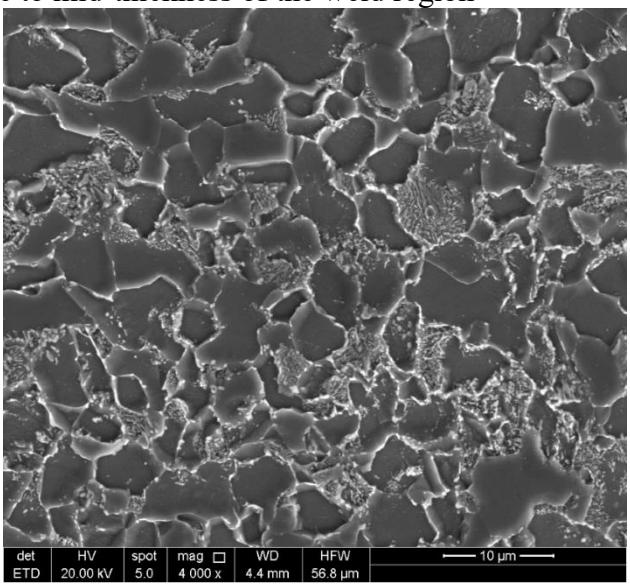

(e) SEM micrograph of ICHAZ close to mid-thickness of the weld region

Figure 13. Microstructures of FGHAZ and ICHAZ.

The RH WM region between the two weld passes is an approximately 1.2 mm wide curved band (Figure 14a). The RH-WM displayed completely reheated microstructure (Figure 14b-e), i.e., equiaxed fine ferrite grains and small amount of tempered bainite and/or martensite, in contrast to the as-deposited coarse columnar WM structure (Figure 11).

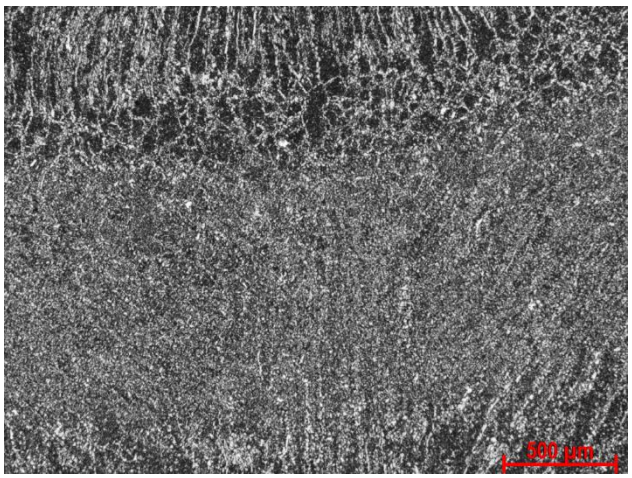

(a) The second-pass weld and RH-WM close to the weld centerline

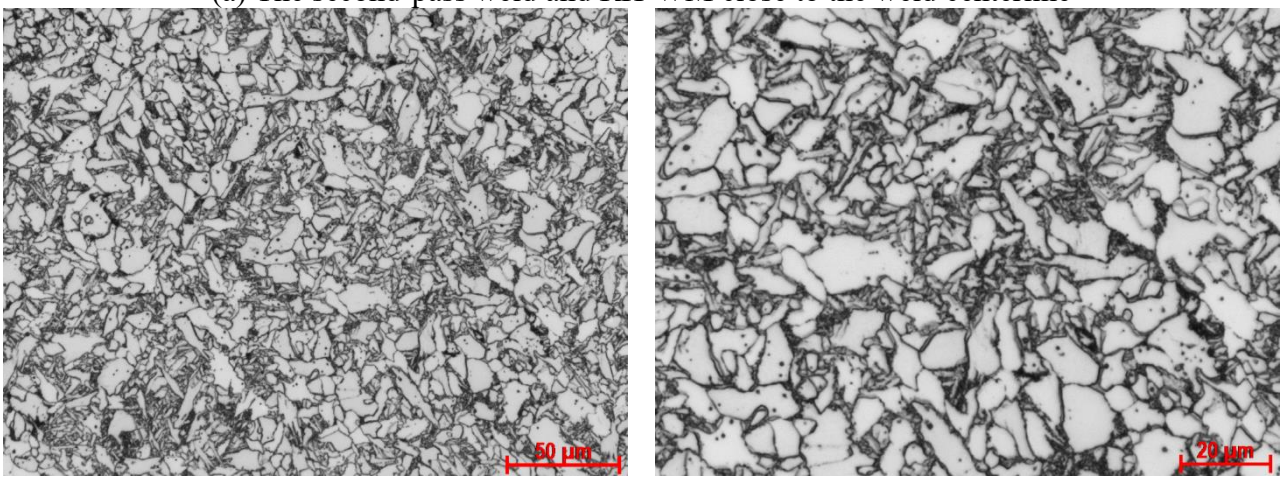

(b) RH WM at the centerline

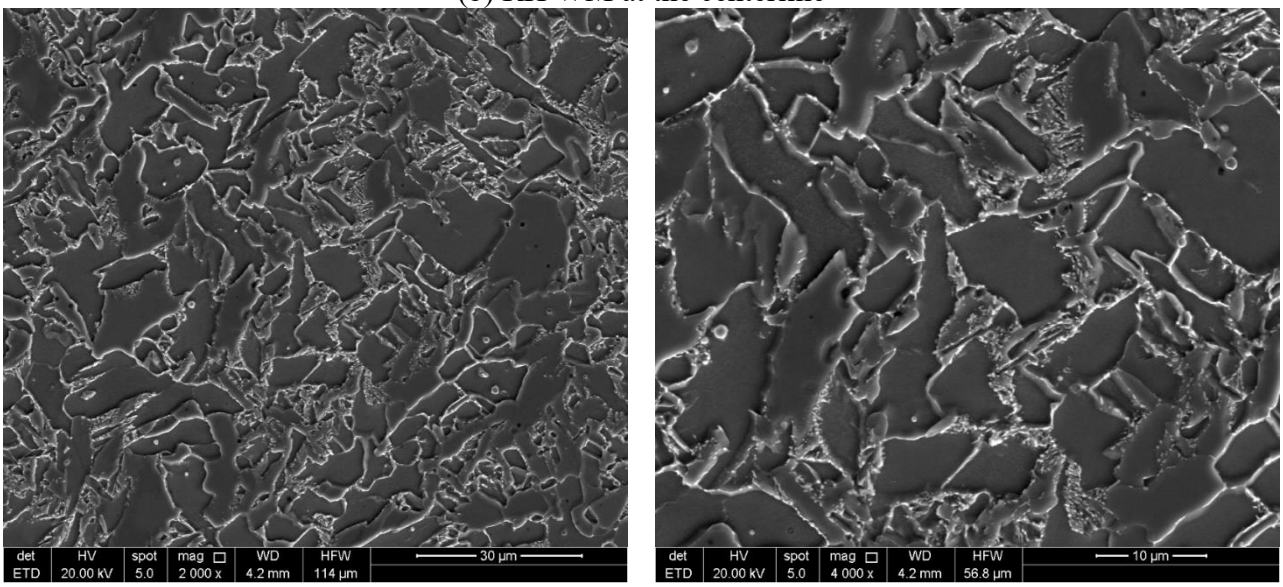

(c) RH WM at the centerline

Figure 14. Microstructure of RH-WM.

In summary, the microstructure of both WM and HAZ showed typical feature of C-Mn steel associated with SAW. However, it is worth noting that very limited volume percentage of acicular ferrite was formed in the weld metal and very significant austenite grain growth occurred in the CGHAZ region, which indicated that SAW was carried out with relatively high heat input. Volume fraction of acicular ferrite was found important for good fracture toughness of C-N steel SAW welds [13]. The welding procedure specification for manufacturing the tank car is needed in order to better understand the relationship between welding parameters, filler alloy composition and microstructure of weld metal.

3.4 Tensile Properties

According to AAR specification [3], all-weld-metal-tension tests are used to measure the strength and ductility of the weld metal while cross-weld tension tests (or joint-tension test) are employed to measure only the strength of the weld joint. In this work, both rectangular (Figure 3) and cylindrical (Figure 4) cross-weld tension specimens were used to measure strength and examine failure characteristics of a current TC128B circumferential weld joint at different temperatures. For cylindrical tensile specimens (Figure 3), the specimens sampled the mid-thickness portion of the weld, i.e., the second-pass weld metal and some RH-WM. The AAR specification requires that the joint specimen breaks in the BM outside the weld and strength is not more than 5% below the specified ultimate tensile strength of TC128B (UTS) (i.e., 560 MPa at room temperature) [3].

Two AWM tests showed very repeatable results. Representative stress-strain curves of the TC128B AWM and BM specimens are shown in Figure 15. AWM specimens showed higher flow stresses and lower elongation than those of the BM specimens and also displayed discontinuous yield up to approximately 1.5% strain.

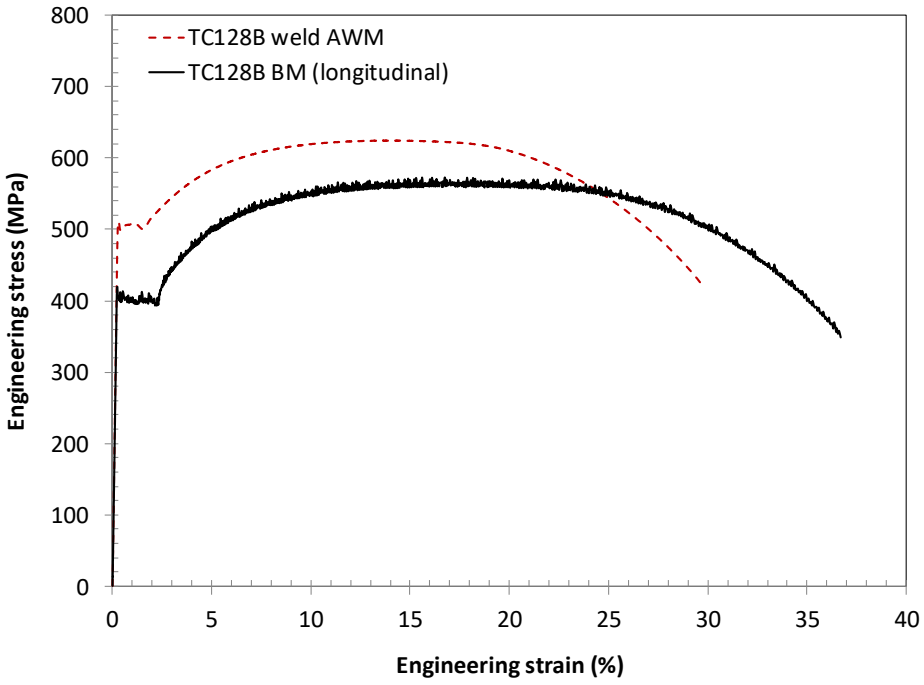

(a) Engineering stress-strain curve

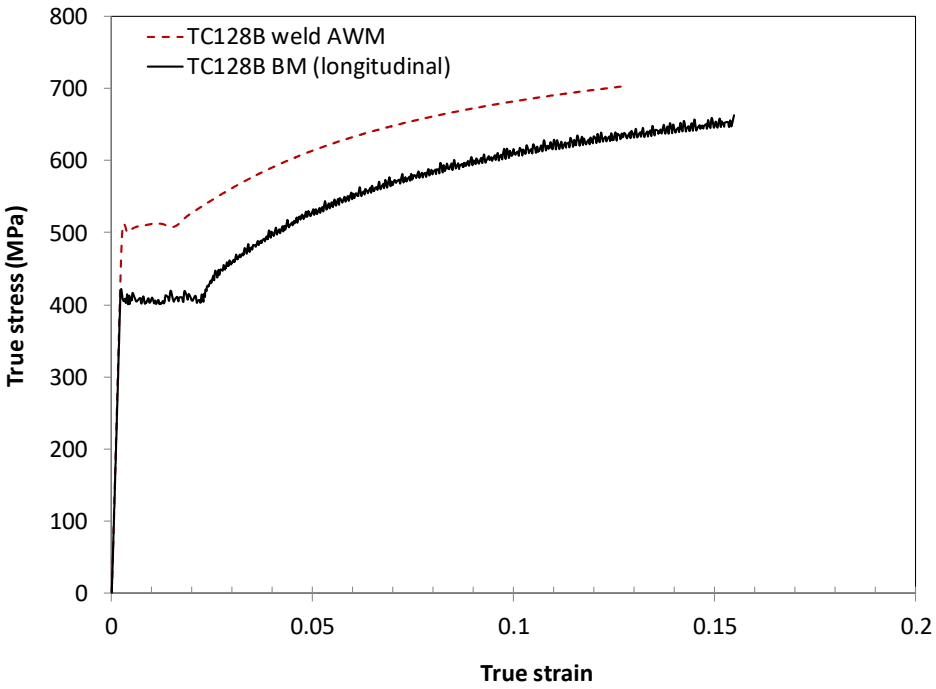

(b) True stress-strain curve

Figure 15. Stress-strain curve of TC128B AWM and BM.

Two full-thickness rectangular tensile specimens were tested at 23°C and the specimens broke in the BM outside of the weld. The UTS values of the rectangular tensile specimens (average, 572 MPa) are essentially the same as those of BM and higher than the minimum UTS of 560 MPa in AAR specification for TC128B [3]. Figure 16 shows nominal stress-strain curves of the weld specimens and that of BM. Cross-weld tensile specimens including the full-thickness ones showed shorter discontinuous regions and higher yield strength than the BM. The strain along the gauge length in a cross-weld tensile specimen is not uniform due to the presence of the hard weld therefore the stress-strain curve can only be considered as a nominal stress-strain curve for information and comparison to the BM. (Note that the nominal strains of cylindrical cross-weld tensile specimens were deduced from the machine grips displacement and corrected to match the elastic stress-strain of steel.) When one examines these tensile stress-strain curves it should also be noted that the rectangular and cylindrical cross-weld tensile specimens had a gauge length of 50 mm, longer than that of the cylindrical BM specimen of 25 mm [4], and the total failure elongation of a longer gauge-length specimen is usually smaller than that of a shorter gauge length.

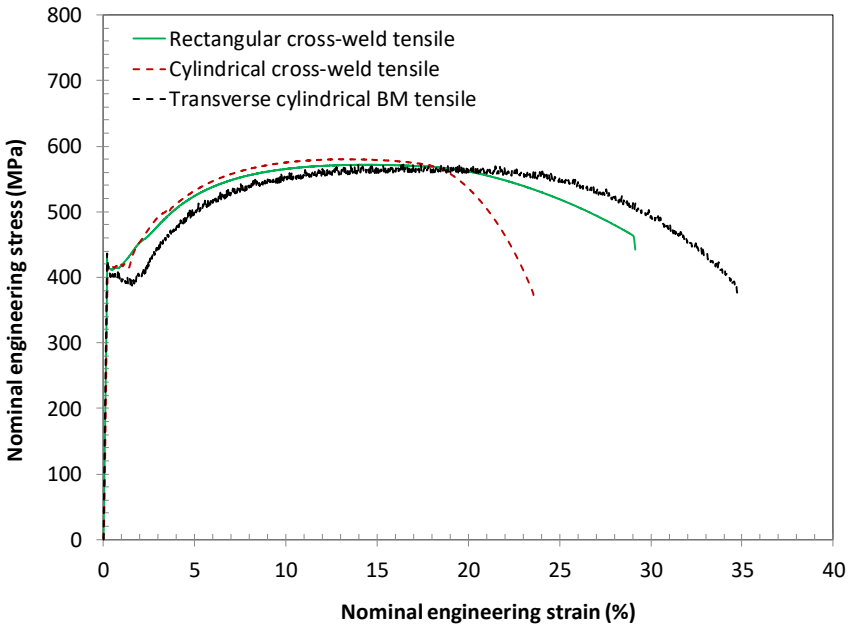

Figure 16. Nominal stress-strain curves of the weld specimens and that of BM.

Tensile test results of TC128B circumferential weld are summarized in Table 2; average tensile properties of the TC128B BM are also provided in Table 2. The UTS of cross-weld specimens decreased with increasing temperature as shown in Figure 17. The UTS of cross-weld tensile specimens dropped sharply beyond 600°C. Photographs of cylindrical tensile specimens are shown in Figure 18. Note that the white lines inserted in Figure 18 are separating WM based on visual observations. All cross-weld specimens tested at 700°C and below failed in the BM. Two of the specimens tested at 700°C and one specimen tested at 800°C broke close to the weld region. Two cross-weld tensile specimens at 800°C failed in the WM. At 850°C, cross-weld tensile specimens failed in the BM. This indicates that the WM may become a weak link for rupture at high-temperatures approximately above 700°C to 800°C. However, it has been noted that in all cases, the UTS of three specimens were similar no matter where the specimen failure locations were located. Futher confirmation of another weld (i.e., a longitudinal weld) would be needed to generalize the observation.

Table 2. Tensile properties of TC128B steel [2,4] and weld specimens

Material	Orientation/Specimen	T (°C) (Specimen #)	σ_y (MPa)	σ_{UTS} (MPa)	E.L. in 25 mm (%)	Failure Location
Steel	RD/cylindrical	-40 (avg.)	437	626	37	Normal (i.e., within specimen gauge)
	RD/cylindrical	23 (avg.)	390	574	37	
	TD/cylindrical	23 (avg.)	389	573	35	
	RD/cylindrical	400 (avg.)	256	481	39	
	RD/cylindrical	600 (avg.)	173	212	61	
	RD/cylindrical	800 (avg.)	58	87	85	
All-Weld-Metal	Along weld/ cylindrical	23 (#1)	497	624	27	
		23 (#2)	500	625	30	
Circumferential Weld	Transverse/rectangular	23 (#1)	-	572	-	BM
		23 (#2)		572		BM
	Transverse/cylindrical	23 (#1)	-	581	-	BM
		23 (#2)		579		BM
		23 (#3)		580		BM
		400 (#1)		476		BM
		400 (#2)		478		BM
		400 (#3)		477		BM
		600 (#1)		204		BM
		600 (#2)		203		BM
		600 (#3)		205		BM
		700 (#1)		97		BM
		700 (#2)		98		BM
		700 (#3)		97		BM
		800 (#1)		75		WM
		800 (#2)		74		WM
		800 (#3)		74		BM
		850 (#1)		64		BM
		850 (#2)		64		BM
		850 (#3)		65		BM

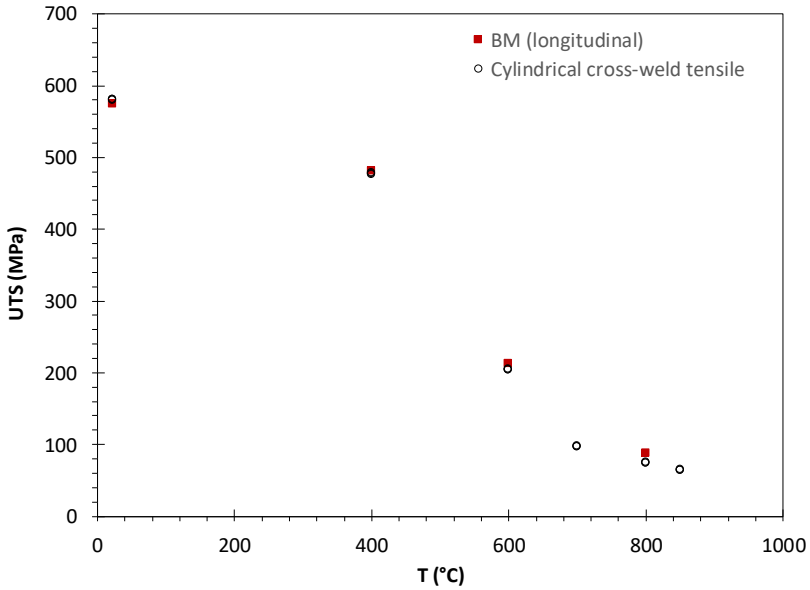

Figure 17. UTS vs. temperature of cross-weld tensile specimens of TC128B circumferential weld.

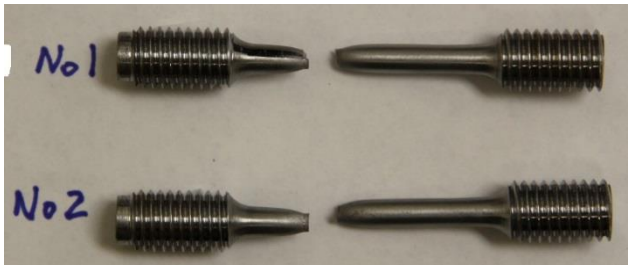

(a) All weld-metal specimens at 23°C

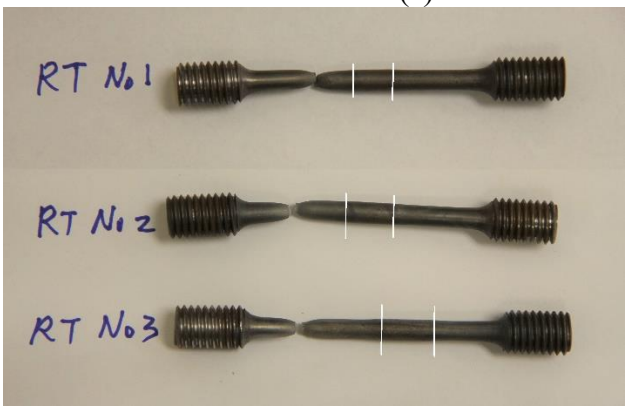

(b) Cross-weld specimens at 23°C

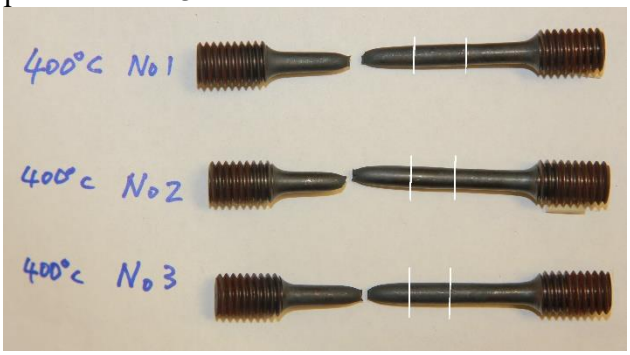

(c) Cross-weld specimens at 400°C

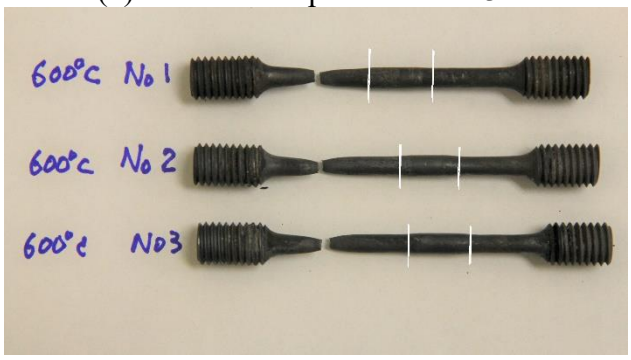

(d) Cross-weld specimens at 600°C

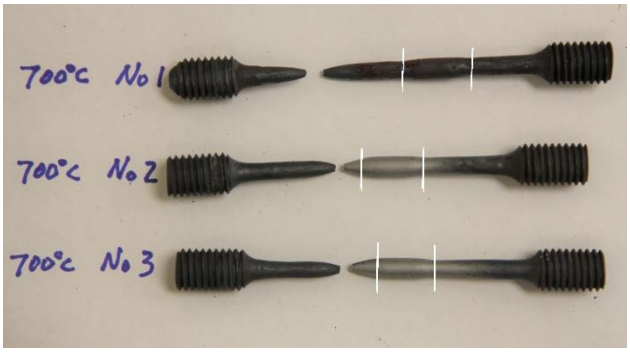

(e) Cross-weld specimens at 700°C

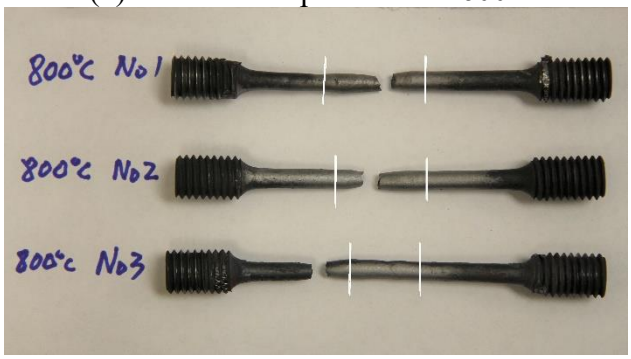

(f) Cross-weld specimens at 800°C

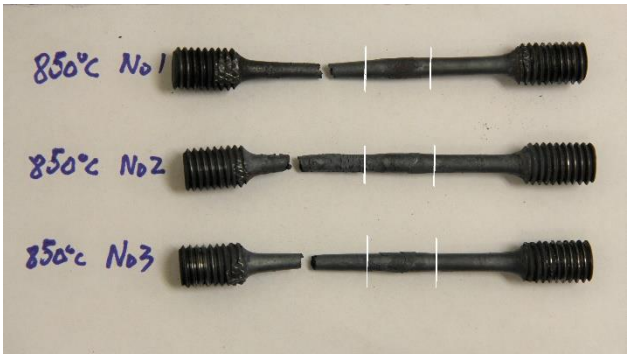

(g) Cross-weld specimens at 850°C

Figure 18. Photographs of cylindrical tensile specimens. White lines indicate approximate weld region in cross-weld specimens.

It is not known how the temperature and exposure time influeced the microstructure and tensile properties of TC128B weld. It has been reported that effect of exposure time up to 120 min on microstructure and tensile properties at temperatures up to 677°C were negligible [14].

3.5 Charpy Impact Properties

Charpy impact toughness is the only toughness requirement included in the AAR tank car steel specifications. Charpy impact tests are also used to evaluate welding procedures for low-temperature applications [3]. The objective of this work was to establish Charpy transition toughness curves of a current TC128B circumferential weld joint and to compare the weld toughness to base steel toughness. Charpy absorbed energy (CVN) values of TC128B circumferential weld are given in Table 3. Charpy transition curves including that of the BM are shown in Figure 19 and the fitting curves are of the form $CVN = C_1 + C_2 \tanh\left(\frac{T - T_0}{C_3}\right)$ (where C_1, C_2, C_3 and T_0 are constants) [4]. CVN of WM were significantly lower than those of BM. CVN of HAZ specimens were between those of BM and WM at temperatures above -40°C, and displayed larger scatter than those of BM and WM because the HAZ specimens sampled inhomogeneous materials (Figure 5b and Figure 6).

For low-temperature applications, the AAR specification [3] requires CVN to be 20.3 J minimum average for three specimens, with a 13.6 J minimum for any one specimen, at -46°C. CVN values for weld centerline specimens at -46°C (average: 18 J, individual: 16 J, 24 J, 13 J) indicated that the weld toughness values were slightly lower than the specification requirement. A close up of Figure 19 showing the low temperature weld results and the AAR specifications is provided in Figure 20. At -46°C, the average CVN of HAZ specimens was 32 J meeting the AAR specification. The low CVN of the circumferential weld may be due to high carbon and oxygen contents, and coarse proeutectoid ferrite and less acicular ferrite than the normal SAW welds [13]. Other possible reasons include that welding procedure specification (WPS) of SAW gives only marginal toughness over the required toughness, variations in welding parameters during welding operation, filler wire and flux composition changes, and moisture control. Since oxygen content above 0.055% (550 ppm) generates many oxide inclusions [6], the oxygen level of 0.0826% of the weld can provide many potential cleavage initiation sites from oxides partially responsible for the observed low CVN. Charpy impact toughness of current TC128B welds deserves further experimental investigation.

The CVN energy of the WM is much lower than that of the BM across all temperatures, as shown in Figure 19. This means that in an accident involving impact the weld is most likely the failure location. Improving the toughness of the weld metal would reduce the chance of fracture/rupture under all service conditions. Weld toughness can be improved by adjusting the welding process, the filler metal, and the post weld heat treatment. It is recommended that a study be conducted to develop an improved weld process that increases weld toughness. The study should be conducted using equipment and processes consistent with what is currently used by industry. It may be possible to greatly improve the weld integrating with no, or little additional cost to the manufacturer.

CMAT recommends testing additional welds from this tank car and others to determine whether low weld toughness is an isolated or systemic issue.

Table 3 Charpy absorbed energy (CVN) of TC128B circumferential weld: average (and individual)

T (°C)	CVN (J)	
	WM	HAZ
25	80 (102,69,69)	208 (232,145,248)
-20	26 (20,28,30)	109 (159,92,75)
-46	18 (16,24,13)	32 (16,17,64)
-60	9 (10,9,9)	92 (120,142,152,66,16,53)
-80	6 (5,7,5)	21 (25,33,6)

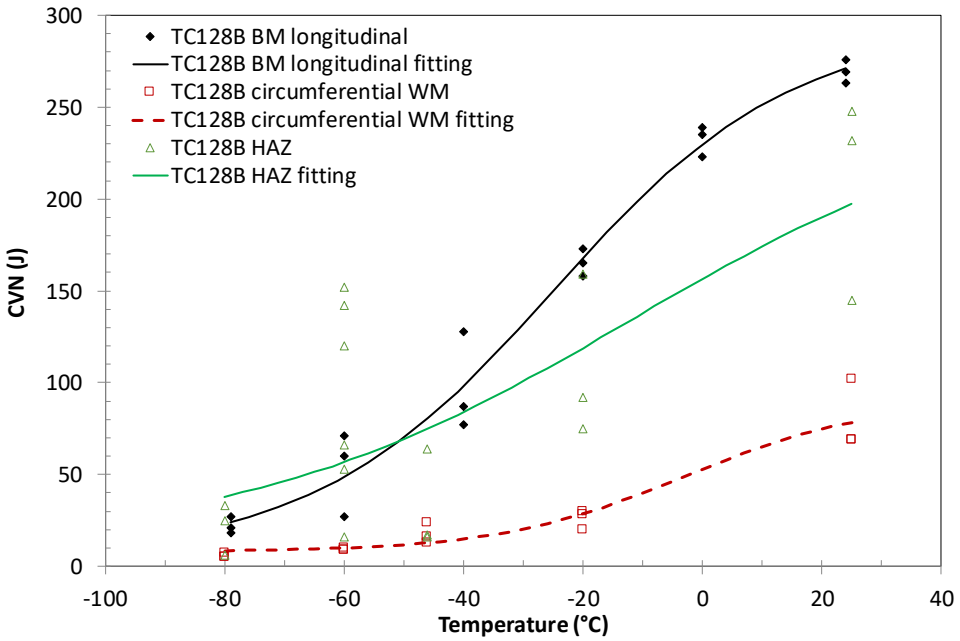

Figure 19. Charpy transition curve of TC128B BM, WM and HAZ.

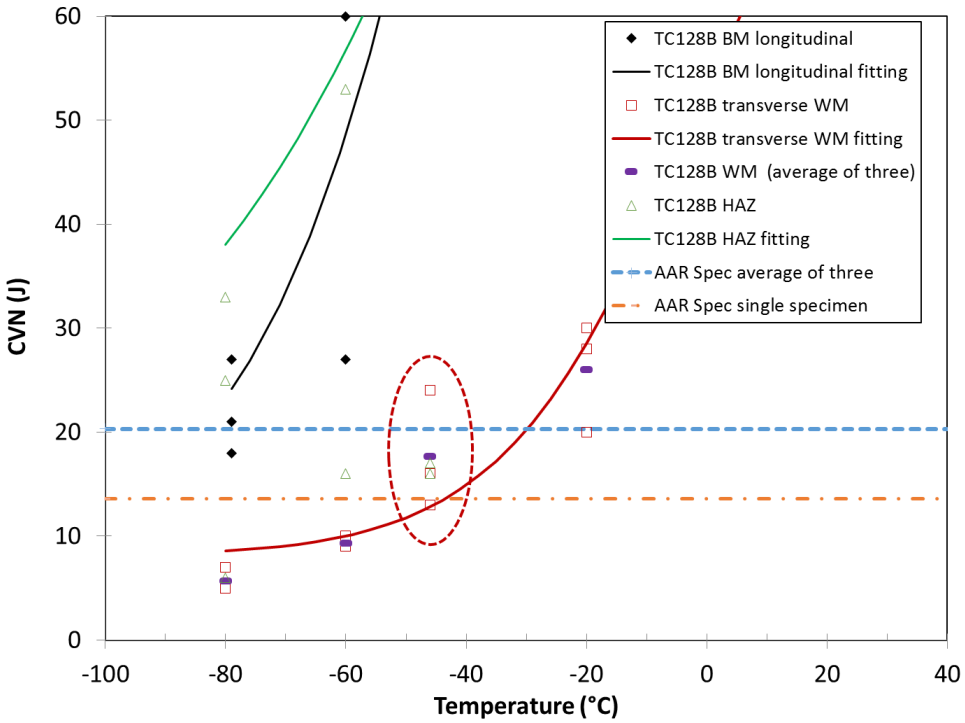

Figure 20. Charpy transition curve of TC128B showing close up of weld metal results at low temperatures. The blue and orange curve show the AAR minimum allowable CVN energy for the average of three and single tests respectively.

4. RECOMMENDED FUTURE WORK

The following areas are recommended for further work based on the results obtained in this project.

Recommended tasks for next fiscal year:

- Develop new welding procedure or modify current welding procedure specification to increase weld metal high temperature strength and improve WM microstructure and CVN results for TC128B.
- Experimentally establish Charpy ductile-to-brittle transition curve of a current TC128B longitudinal weld for damage tolerance assessment and compliance with the AAR specification
- Experimentally establish Charpy ductile-to-brittle transition curve for other tank car welds if material is available.
- Perform creep tests of cross-weld specimens of a current TC128B circumferential weld.
- Perform in-depth microstructural examinations of tested cross-weld specimens of BM and WM at 800-850°C using transmission electronic microscope (TEM) and other methods.
- Characterize and perform high-temperature cross-weld tensile tests of a current TC128B longitudinal weld. Analyze chemical compositions of TC128B welds.
- Perform J/CTOD tests at low temperatures (23°C, -20°C and -46°C) to characterize fracture initiation toughness at low temperatures of a TC128B circumferential weld.
- Perform J/CTOD tests at low temperatures (-20°C and -46°C) to characterize fracture initiation toughness at low temperatures of A516-70 and TC128B steels.

- Perform CTOA/DWTT tests at low temperatures (-20°C and -46°C) to characterize fracture propagation toughness to demonstrate suitable fracture propagation resistance at low temperatures of A516-70 and TC128B steels. The results can also be used to compare Charpy and DWTT results both in terms of the effects of thickness (i.e. DWTT is used in the pipeline industry primarily to characterize full-thickness properties) and temperature.
- Determine effects of pre-deformation on properties for A516-70 plate (e.g., deformation during forming operation).
- Obtain tank car steels from at least two other sources to obtain a comprehensive dataset.

CONCLUSIONS

A current TC128B circumferential weld was characterized and tested. The main conclusions are

- The weld was made using a double pass procedure. The first-pass (or root pass) weld was made from the inside surface and the WM height was about 1/3 of the weld thickness while the second-pass (or cap pass) weld completed the joining. The combined weld and HAZ widths were approximately 14.8 mm close to the mid-thickness (the smallest), 22 mm at the inside surface and 24 mm at the outside surface (the largest), respectively, which are within normal ranges. The HAZ width ranged approximately 2.3-4.2 mm. WM and HAZ showed various and typical microstructures.
- The hardness values in the weld and HAZ were considerably higher than those of BM, i.e., demonstrating desired weld strength over-matching. The average and standard deviation of micro-hardness of BM, HAZ and WM were 164±8 (from 152 to 182), 191±17 (from 151 to 217) and 194±9 (from 163 to 217), respectively.
- All-WM specimens tested at 23°C showed that the weld was made to the strength specification and the weld was stronger than the steel.
- UTS of cross-weld tensile specimens dropped sharply beyond 600°C. All cross-weld specimens tested at 700°C and below failed at BM. Two of the spcimens tested at 700°C and one specimen tested at 800°C broke close to the weld region. Two cross-weld tensile specimens at 800°C failed at WM. At 850°C, cross-weld tensile specimens failed in BM. These indicated that the WM may become a weak link at high-temperatures approximately above 700°C to 800°C.
- CVN values of WM were significantly lower than those of BM. CVN values of HAZ specimens were between those of BM and WM at temperatures higher than -40°C, and displayed larger scatter. CVN values for WM specimens at -46°C (average: 18 J, individual: 16 J, 24 J, 13 J) indicated that the weld toughness values were slightly lower than the specified values or at the borderline.

ACKNOWLEDGEMENTS

This work was funded by Transport Canada's Transportation of Dangerous Goods Directorate under the guidance of Mr. Ian Whittal and Mr. Michael Spiess. We would like to gratefully acknowledge Dr. F. Fazalli for useful discussions on microstructure in the weld region, Ms. P. Liu for performing metallography and micro-hardness, Ms. R. Zavadil for SEM examination and Ms. L. Yang for photography of tested tensile specimens. Dr. Jason Lo, Program Manager, is gratefully acknowledged for his review of the report.

REFERENCES

1. S. Xu, "A Review of the Strength and Fracture Toughness Properties of Two Tank Car Steels: TC128B and A516-70", CanmetMATERIALS Report, CMAT-2016-WF 8933792, May 2016.
2. C.H.M. Simha and J. Mckinley, "High-Temperature Mechanical Properties of Tank Car Steel – Testing and Analysis", CanmetMATERIALS Report, CMAT-2017-WF 15390827, November 2017.
3. AAR Manual of Standards and Recommended Practices, Section C-III (Appendix M, M-1002, and Annex W), "Specifications for Tank Cars", 2014.
4. S. Xu, J. Liang, L. Yang, A. Laver and W.R. Tyson, "Tensile and Fracture Toughness of a Current Tank Car Steel, TC128B", CanmetMATERIALS Report, CMAT-2017-WF 16144032, May 2017.
5. ASTM A20/A20M-15, "Standard Specification for General Requirements for Steel Plates for Pressure Vessels", ASTM International, 100 Barr Harbor Drive, PO Box C700, West Conshohocken, PA 19428-2959, United States, November 2015.
6. J. Amanie, "Effect of Submerged Arc Welding Parameters on the Microstructure of SA516 and A709 Steel Welds", PhD Thesis, Department of Mechanical Engineering, University of Saskatchewan, Saskatoon, Canada, August 2011. (https://harvest.usask.ca/bitstream/handle/10388/ETD-2011-07-42/AMANIE-DISSERTATION.pdf?sequence=3&isAllowed=y)
7. M.A. Sutton, I. Abdelmajid, W. Zhao, D. Wang and C. Hubbard, "Weld Characterization and Residual Stress Measurements for TC-128B Steel Plate", Journal of Pressure Vessel Technology, Vol. 124, 2002, pp. 405-414.
8. J.A. Gianetto, D.M. Mak, R. Bouchard, S. Xu, and W.R. Tyson, "Characterization of the Microstructure and Toughness of DSAW and ERW Seam Welds of Older Linepipe Steels", Proc.4th International Pipeline Conference (IPC2002), Calgary, Alberta, Canada, Sept. 29-Oct. 4, 2002, ASME, Paper IPC02-27157, pp.1-12.
9. J.A. Francis, W. Mazur and H.K.D.H. Bhadeshia, "Review Type IV Cracking in Ferritic Power Plant Steels", Materials Science and Technology, Vol. 22, 2006, pp. 1387-1395
10. S. L. Mannan and K. Laha, "Creep-Behavior of Cr-Mo Steel Weldments", Transactions of the Indian Institute of Metals, Vol. 49, 1996, pp. 303–320.
11. G.E. Hicho, "The Mechanical, Stress-Rupture, and Fracture Toughness Properties of Normalized and Stress Relieved AAR TC128 Grade B Steel at Elevated Temperatures", Report NISTIR 5157, March 1993.
12. G.E. Hicho and D.E. Harne, "Weld and Heat Affected Zone Crack Arrest Fracture Toughness of AAR TC128 Grade B Steel", NISTIR 4767, Report No. 25, NIST, February 1992.

13. L.E. Svensson and B. Gretoft, “Microstructure and Impact Toughness of C-Mn Weld Metals”, Welding Research Supplement, December 1990, pp. 454-s - 461-s.
14. G.E. Hicho, “The Mechanical, Stress-Rupture, and Fracture Toughness Properties of Normalized and Stress Relieved AAR TC128 Grade B Steel at Elevated Temperatures”, Report NISTIR 5157, Report No. 26, NIST, March 1993.